CHEMISTRY OF MATERIALS

pubs.acs.org/cm

Article

Infrared Nonlinear Optical Polymorphs α- and β-$SrCu_2SnS_4$ Exhibiting Large Second Harmonic Generation Responses with Requisite Phase-Matching Behavior

Ya Yang, Kui Wu,* Bingbing Zhang,* Xiaowen Wu, and Ming-Hsien Lee

Cite This: *Chem. Mater.* 2020, 32, 1281−1287

Read Online

ACCESS | Metrics & More | Article Recommendations | Supporting Information

ABSTRACT: α- and β-$SrCu_2SnS_4$ polymorphs, exhibiting special structural changes and excellent physicochemical performances, were successfully synthesized and characterized as promising IR NLO candidates. Note that they satisfy the essential phase-matching condition and have strong SHG responses about 0.7 and 1.0 times those of benchmark $AgGaS_2$ under 2.09 μm incident light, respectively, which agree well with the theoretical SHG coefficients and suitable birefringences based on first-principles calculation. Moreover, it is also verified that their SHG effects originate from the synergetic contribution between CuS_4 and SnS_4 ligands after the SHG density calculations.

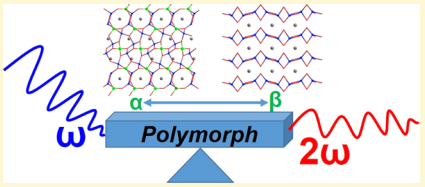

Inorganic functional materials have been widely explored in recent decades and applied in many key technology regions because of their multiple structures and attractive performances, especially for the laser frequency conversion.[1−20] Metal chalcogenides exhibit red-shifted stretching frequencies and high polarizability than oxides that are more beneficial for infrared laser application.[21−35] As for polymorphism, they adopt identical chemical compositions but special structural changes, providing an effective route to study the relationship between structure and performance.[36−40] So far, numerous polymorphs have been discovered in the quaternary diamond-like semiconductors (DLSs), such as the typical I_2−II−IV−Q_4 (I = monovalent cations; II = bivalent cations; IV = Si, Ge, Sn; Q = S, Se) DLSs system.[41] Note that several of them undergo an interesting change in the coordination of tetrahedral stacking and show potential application as infrared nonlinear optical (IR NLO) materials with excellent physicochemical properties. For instance, both Cu_2ZnSiS_4 polymorphs (α: $Pmn2_1$ and β: Pn) display good second harmonic generation (SHG) responses (1.2 × benchmark $AgGaS_2$) under 1.55 μm incident light;[42] besides, α- and β-Li_2MnSnS_4 ($Pna2_1$ vs Pn) have moderate SHG effects of about 0.4 × $AgGaS_2$@2.1 μm.[43] Except for the above-mentioned DLS system, multiple structural changes also appeared in the similar I_2−Ba/Sr/Pb/Eu−IV−Q_4 system with different IV or VI atoms and only one polymorph, $Cu_2BaSnSe_4$ (α: $P3_22_1$ vs β: $Ama2$), was found in the above system.[44−46] A detailed literature survey indicates that different sintering temperatures or starting ingredients are in favor of producing various coordination environments of structural ligands, and these structural modifications proceed extremely slowly, leading to the preservation of a metastable phase in view of their high energy barriers. Based on the above analysis, in this work, other polymorphs, α- and β-$SrCu_2SnS_4$ (α: $P3_22_1$ vs β: $Ama2$), were successfully synthesized, and these polymorphisms are the first discovered examples of the I_2−Sr−IV−VI_4 system. Both of them exhibit good SHG responses that are about 0.7 and 1.0 times the benchmark $AgGaS_2$ and satisfy the phase-matching demand, indicating that they can be expected as promising IR NLO candidates. The first-principles calculation also verifies that the calculated results (NLO coefficients and birefringence) are in agreement with the experimental values. Meanwhile, the combined contribution of CuS_4 and SnS_4 ligands achieves the origin of their large SHG responses by means of the SHG density calculations.

Single-crystal X-ray diffraction test shows that they crystallize in the $P3_22_1$ space group of the trigonal system for α-phase and orthorhombic $Ama2$ for β-phase (Tables S1 and S3). The α-phase was discovered in 1976 by Teske, but its critical NLO properties have not been reported.[47] Note that the β-phase has been successfully synthesized for the first time. Herein, we have systematically studied the structural modifications between the two phases. As for the α-phase, its asymmetric unit is composed of one Sr, one Sn, two Cu, and four S atoms. In its structure, CuS_4 units with d(Cu−S) = 2.278−2.407 Å connect together by sharing corners and edges to form three types of 3D channels including 4-member ring (4-MR), 8-MR, and 12-MR (Figure 1a), and then further link with SnS_4 ligands (d(Sn−S) = 2.375−2.397 Å) to surround the roughly circular 3D channels in which Sr atoms are located (Figure 1b,c). From another point of view, SrS_8 dodecahedra also link with each other to form irregular 3D tunnels, where Cu and Sn atoms are located (Figure 1d). As for the β-phase,

Received: November 22, 2019
Revised: January 19, 2020
Published: January 21, 2020

https://dx.doi.org/10.1021/acs.chemmater.9b04842
Chem. Mater. 2020, 32, 1281−1287

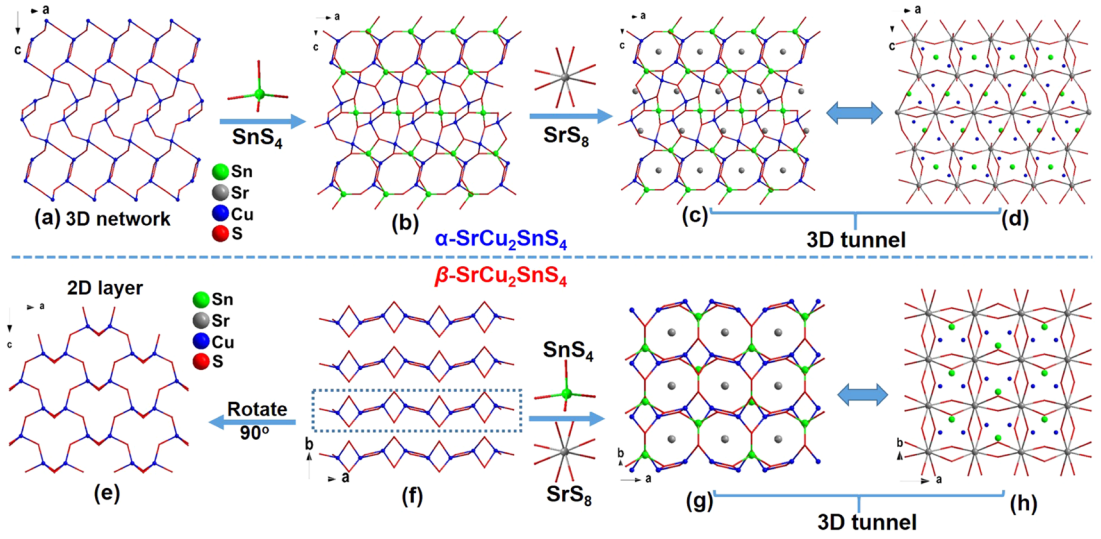

Figure 1. Structural modifications between α- and β-$SrCu_2SnS_4$. α-Phase: (a) 3D network formed by CuS_4 ligands; (b) combination of CuS_4 and SnS_4 ligands; (c) structure view from the *b*-axis (Sr−S bonds were omitted); and (d) structure view from the *b*-axis (Cu−S and Sn−S bonds were omitted). β-Phase: (e) 2D layer formed by CuS_4 ligands; (f) 2D layers stacked along the *b*-axis; (g) 3D network structure (Sr−S bonds were omitted); and (h) 3D network formed by SrS_8 ligands (Cu−S and Sn−S bonds were omitted).

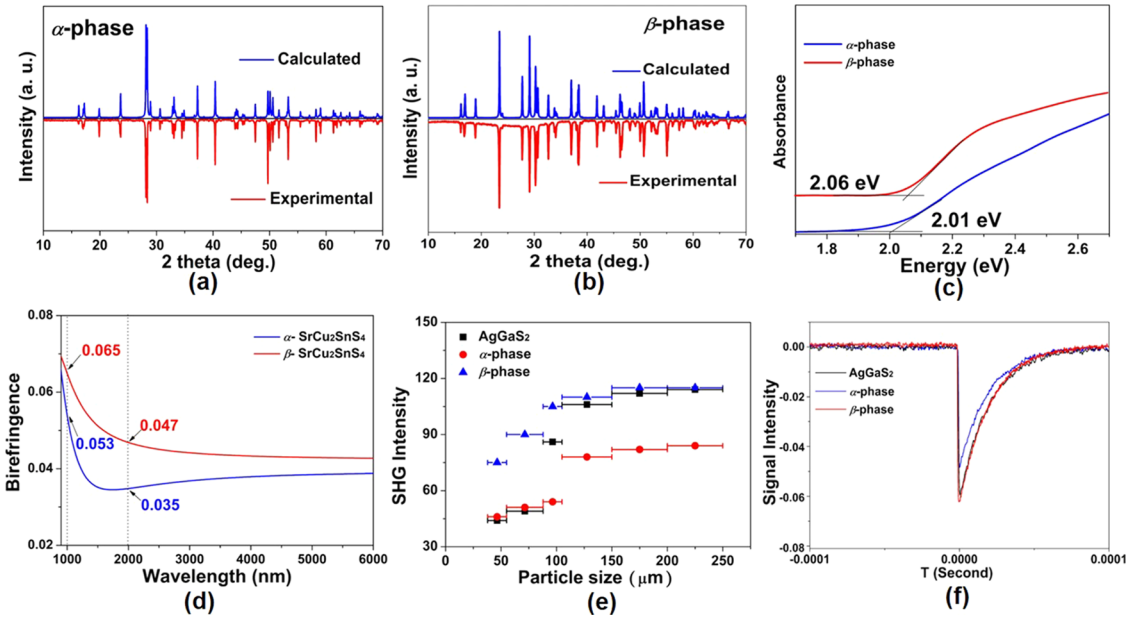

Figure 2. (a, b) PXRD patterns. (c) Experimental band gaps. (d) Birefringence versus wavelength. (e) Curves of SHG response versus particle size ($AgGaS_2$ as the reference). (f) SHG signals (volt) diagram of title crystals and $AgGaS_2$.

2D layers composed of corner- and edge-sharing CuS_4 ligands with d(Cu−S) = 2.314−2.503 Å stack along the *b*-direction, which are different from the 3D network found in the α-phase (Figure 1e). Adjacent $(CuS_4)_n$ layers are interconnected by isolated SnS_4 ligands with d(Sn−S) = 2.377−2.415 Å to compose 3D regular tunnels along the *c*-axis; similarly, SrS_8 dodecahedra are also interlinked together to form regular 3D tunnels, which is also different from the irregular 3D network in the α-phase (Figure 1f−h). Survey on the I_2−Sr/Ba−IV−Q_4 system shows that these compounds undergo multiple structural changes with different IV or Q atoms, such as orthorhombic to trigonal (*Ama*2 to $P3_22_1$ or $P3_12_1$),[44] orthorhombic to tetragonal (*I*222 to $I\bar{4}2m$),[48] and tetragonal to trigonal ($I\bar{4}2d$ to *R*3*c*).[49] So far, only one polymorphism, $Cu_2BaSnSe_4$ (α: $P3_22_1$ vs β: *Ama*2), was found in the above system, which is similar to that in title compounds. Extending the survey to the I_2−II−IV−Q_4 DLSs system shows that seven polymorphs were discovered and show various structural changes including monoclinic to orthorhombic (Cu_2ZnSiS_4: *Pn* vs $Pmn2_1$),[42] orthorhombic to orthorhombic (Ag_2CdGeS_4: $Pmn2_1$ vs $Pna2_1$),[50,51] orthorhombic to tetragonal (Cu_2ZnGeS_4: $Pmn2_1$ vs $I\bar{4}2m$),[52,53] and tetragonal to tetragonal (Cu_2ZnSnS_4: $I\bar{4}2m$ vs $I\bar{4}$)[54,55] (Table S2). A comparison of their structures shows that the direction of the arrangement of IQ_4 units is obviously different, leading to the structural transformation and further inducing multiple phases.[56] Based on different space groups ($Pmn2_1$, *Pn*, $Pna2_1$, $I\bar{4}2m$, and $I\bar{4}$), five kinds of structural changes on the link modes of monovalent-cation-centered tetrahedral ligands exist; for instance, a 2D layer, comprising monovalent-cation-

https://dx.doi.org/10.1021/acs.chemmater.9b04842
Chem. Mater. 2020, 32, 1281−1287

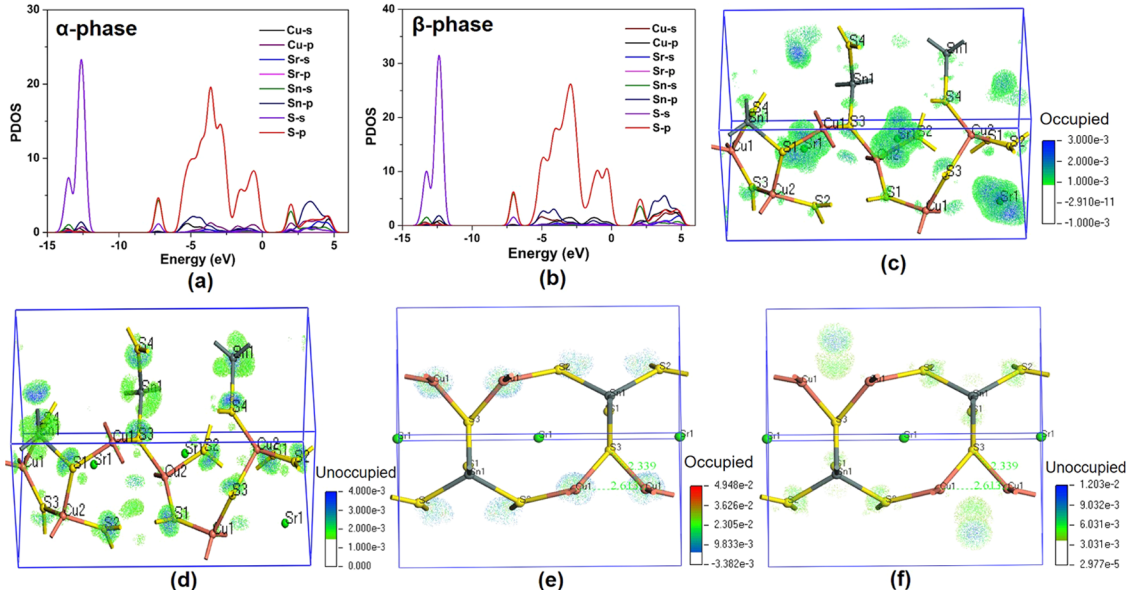

Figure 3. (a, b) Partial density of states (PDOS) for title crystals. (c, d) SHG density of α-phase at the occupied and unoccupied states. (e, f) SHG density of β-phase at the occupied and unoccupied states.

centered tetrahedral ligands by corner-sharing S atoms, located at the *ac*-plane in $Pmn2_1$; a 3D framework structure, comprising six-tetrahedra surrounded channels, located at the *bc*-plane in *Pn*; 3D framework structure, comprising eight-tetrahedra surrounded channels, located at the *ab* plane in $Pna2_1$; tetrahedral-formed 2D layer located at the *ab* plane in $I\bar{4}2m$; and disordered atomic occupations in the $I\bar{4}$. As for the $Cu_2-Sr-IV-Q_4$ system, four compounds were discovered including $SrCu_2M^{IV}Q_4$ (IV = Ge, Sn; Q = S, Se) that crystallize in two different space groups: *Ama*2 vs $P3_221$.[57,58] In other words, α- and β-$SrCu_2SnS_4$ can be viewed as the first discovered polymorphism in the $I_2-Sr-IV-VI_4$ system. Based on the above analysis, the arrangement modes of d^{10}-element-centered tetrahedra may produce an enormous effect on regulating the phase transition, which also gives us a good inspiration to design and predict new polymorphisms.

Title crystals with red color were prepared by the spontaneous crystallization method in vacuum-sealed silica tubes (see detail in the SI). Note that their high yields (~95%) were achieved after repeated grinding and calcination. Both of them are stable in the air for several months. Their experimental powder XRD patterns are in agreement with the theoretical data, which ensure the accuracy of the following test results (Figure 2a,b). We have also measured their thermal properties in the vacuum-sealed silica tubes (Figure S1). As for the orthorhombic phase (β), its melting and crystallization temperatures are 771 and 741 °C, respectively, and no phase-transformation phenomenon has been found in its DSC curve. Besides, we have also measured their PXRD patterns at four different sintering temperatures (700, 800, 900, and 1000 °C) for previously prepared orthorhombic phase samples (Figure S2), and all of them agree well with the theoretical XRD data (β-phase) and no α-phase patterns were observed. Moreover, as for α-phase, its DSC curve shows the melting and crystallization temperatures of 774 and 744 °C, respectively, with the phase transition point (from α- to β-phase) at 672 °C, which is also verified by the experimental PXRD patterns at different sintering temperatures. Note that α-phase is changed to β-phase during the recrystallization process at 700−1000 °C. Thus, it can be concluded that $SrCu_2SnS_4$ exhibits the two polymorphs with phase-transformation temperature from α- to β-phase of 672 °C. As for one IR NLO material, important physicochemical properties including band gap, SHG response, laser damage threshold (LDT), and birefringence should be systematically studied. In this work, based on the polycrystalline samples, their UV−visible diffuse reflectance spectra were recorded and the result shows that the band gaps of α- and β-phases are 2.01 and 2.06 eV (Figure 2c), respectively, which are similar to that of $BaCu_2SnS_4$ (1.96 eV) and still larger than that of commercialized $ZnGeP_2$ or $AgGaSe_2$ crystals.[59,60] Powder laser damage thresholds (LDTs) were also measured under 1.06 μm laser, and title crystals exhibit about 2.3 times that of $AgGaS_2$ (as the reference), which shows that they may sustain the high-power laser radiation and have the potential to be applied in the laser frequency downconversion system under around 1 μm common Nd- or Yb-doped YAG laser irradiation (Table S4).[34] We measured the infrared (IR) spectra for title crystals (Figure S3); it is clear that there were no obvious absorption peaks in the range from 4000 to 500 cm^{-1}, indicating that they exhibit a wide IR transmission region up to 20 μm (500 cm^{-1}). To further analyze the intrinsic effect on material band gaps, we have also calculated their band structures and partial density of states (PDOS) based on the first-principles calculation. Their theoretical band gaps are 1.08 (α: direct band gap) and 1.14 eV (β: indirect band gap), respectively, which are smaller than the experimental values owing to the discontinuity of the exchange-correlation energy in GGA calculation[61] (Figure S4). Besides, both of them also possess similar PDOS diagram (Figure 3a,b). As for β-phase, the region from −15 to −10 eV is mainly occupied by the S 2s and Sn 5s,5p orbitals, with a minor contribution from Cu 4p orbitals. Besides, the range from −7.5 eV to the Fermi level in the valence bands could be considered as the main contribution of S 3p with Cu 4s and Sn 5p orbitals. Also, S 3p and Sn 5s orbitals are the main contributors to the bottom of conduction bands. Therefore, the optical absorption for title crystals originates from the combined action of two anionic groups (CuS_4 and SnS_4). In

https://dx.doi.org/10.1021/acs.chemmater.9b04842
Chem. Mater. 2020, 32, 1281−1287

comparison with those of the previously reported SrA_2SnS_4 (A = Li, Na) well-known analogues,[62] the experimental and theoretical band gaps of title crystals are smaller, which also verifies that the effect of alkali metal atoms on band gap can be negligible and their optical absorptions are only determined by the SnS_4 ligand. To verify the application potential in the IR region, the SHG responses at 2.09 μm fundamental light irradiation for title crystals have been also investigated (Figure 2e,f). With the increase of particle sizes of microcrystalline samples, their SHG intensities show the same increase, indicating that they satisfy the essential phase-matching (PM) condition. Generally, birefringence as a critical parameter can be used to estimate the phase-matching capability and the optional magnitude (Δn) should satisfy the suggested range from 0.03 to 0.10. Herein, we have also calculated their refractive index variation with wavelengths and their birefringences (Δn) were calculated to be 0.053 (α) and 0.065 (β) at 1 μm or 0.035 (α) and 0.047 (β) at 2 μm, respectively, which are well situated within the above limited range and consistent with the experimental PM results (Figure 2d). Besides, in comparison with benchmark $AgGaS_2$, the maximum SHG intensities at 200−250 μm particle sizes are about 0.7 × $AgGaS_2$ for α-phase and 1.0 × $AgGaS_2$ for β-phase, which are comparable to the SHG values of other famous IR NLO crystals, such as $LiInS_2$ (0.56 × $AgGaS_2$),[63,64] $LiGaSe_2$ (0.76 × $AgGaS_2$),[63,65] $LiInSe_2$ (0.9 × $AgGaS_2$),[66] and $BaGa_4S_7$ (1.0 × $AgGaS_2$).[67] We have also calculated the theoretical NLO coefficients for title crystals, and their calculated maximum values are −9.0 pm/V for α-phase and 9.4 pm/V for β-phase, which also match well with the experimental values.

As for the origin of the NLO effect in title crystals, we also used the SHG density calculation to analyze the contribution of anionic ligands. According to the result of SHG density, it can be concluded that their SHG effects originate from the cooperative influence of CuS_4 and SnS_4 tetrahedral groups and the introduction of Cu (or other d^{10}-elements) into crystal structures generates much improvement in NLO performances of IR materials (Figure 3c−f). In view of the polar space group ($Ama2$) for β-phase, dipole moment calculations were also chosen to study the origin of the SHG effect (Table S6). The result shows that the whole dipole moment is 24.81 D for β-phase, and the direction of polarization for all anionic groups in β-phase is along the z-axis, with the other two directions (x and y) canceling out to zero. The dipole moment of each anionic group is about 11.98 D for CuS_4 and 27.6 D for SnS_4, which produce the main role in the SHG effect. Thus, the coupling effect of two anionic groups (CuS_4 and SnS_4) offers the main contribution to the SHG origin of title crystals. Compared with the physicochemical properties of other polymorphisms in the related I_2−II−IV−VI_4 DLSs system, such as Cu_2ZnSiS_4[42] and Li_2MnSnS_4,[43] both the phases exhibit similar band gaps and SHG responses, indicating that structural transitions produce no obvious effect on the NLO performances of polymorphisms (Table S5). Based on the above research, title crystals exhibit strong SHG responses (~0.7 and 1.0 × $AgGaS_2$) with essential PM behavior and large LDTs (2.3 × $AgGaS_2$), indicating them as promising IR NLO crystals (Table 1). We have summarized the optical performances (band gap and SHG effect) of the I_2−Ba/Sr/Pb/Eu−IV−Q_4 system (Table S7).

In summary, new polymorphs, α- and β-$SrCu_2SnS_4$ (α: $P3_221$ vs β: $Ama2$), were successfully synthesized. Structural differences between title crystals were compared, and this structural transition can be considered as the variable arrangement directions of CuS_4 units, which also produce a good inspiration in designing new polymorphisms. An investigation of the physicochemical properties shows that title crystals exhibit excellent performances including reliable chemical stability, strong SHG responses (~0.7 and 1.0 × $AgGaS_2$), high LDTs, required PM behavior, and suitable Δn as promising IR NLO materials in comparison with commercial $AgGaS_2$. An analysis of the origin of SHG effects based on two calculation methods (dipole moment and SHG density) shows that the above two calculated results agree well and the SHG effects of both of them are derived from the synergetic contribution of CuS_4 and SnS_4 anionic groups.

Table 1. Performance Comparison between Title Crystals and $AgGaS_2$ (as the Reference, AGS) Including, d_{ij} as the Calculated NLO Coefficients

compounds	α-phase	β-phase	$AgGaS_2$[63,68]
space group	$P3_221$	$Ama2$	$I\bar{4}2d$
band gap (eV)	2.01	2.06	2.64
SHG response (× AGS)	~0.7	~1.0	1.0
maximum d_{ij} (pm/V)	−9.0	9.4	13.0
LDT (× AGS)	~2.3	~2.3	1.0
birefringence (Δn@1 μm)	0.053	0.065	0.039

EXPERIMENTAL SECTION

Spontaneous crystallization processes of title compounds were completed in the vacuum-sealed silica tubes under different sintering temperatures. Selected high-quality crystals were used for data collection on a Bruker SMART APEX II 4K CCD diffractometer using Mo Kα radiation (λ = 0.71073 Å) at 296 K. Powder X-ray diffraction (XRD) patterns of title compounds were collected on a Bruker D2 X-ray diffractometer with Cu Kα radiation (λ = 1.5418 Å) at room temperature. Diffuse-reflectance spectra were measured by a Shimadzu SolidSpec-3700DUV spectrophotometer in the wavelength range of 200−2600 nm at room temperature. IR spectra of title polymorphs were investigated within the range from 4000 to 400 cm^{-1}. A HCT-2 (HENVEN) thermal analyzer was used to investigate their differential scanning calorimetric (DSC) curves. Powder SHG responses were investigated by a Q-switch laser (2.09 μm, 3 Hz, 50 ns) under six different particle sizes with $AgGaS_2$ as the reference. LDTs of title compounds were evaluated on powder samples (150−200 μm) with a pulsed YAG laser. Electronic structures and theoretical performances were studied by density functional theory (DFT) based on ab initio calculations (details in the Supporting Information).

ASSOCIATED CONTENT

Supporting Information

The Supporting Information is available free of charge at https://pubs.acs.org/doi/10.1021/acs.chemmater.9b04842.

Synthesis, measurements, crystal data, structural comparison, bond valence and GII, LDT, and performance comparisons, DSC curves, PXRD at different temperatures, IR spectra, and band structures of title crystals (PDF)

Datablock 1, ellipsoid plot (ZIP)

AUTHOR INFORMATION

Corresponding Authors

Kui Wu − *Key Laboratory of Medicinal Chemistry and Molecular Diagnosis of the Ministry of Education, Key*

https://dx.doi.org/10.1021/acs.chemmater.9b04842
Chem. Mater. 2020, 32, 1281−1287

Laboratory of Analytical Science and Technology of Hebei Province, College of Chemistry and Environmental Science, Hebei University, Baoding 071002, China; orcid.org/0000-0001-8242-4613; Email: wukui@hbu.edu.cn

Bingbing Zhang − *Key Laboratory of Medicinal Chemistry and Molecular Diagnosis of the Ministry of Education, Key Laboratory of Analytical Science and Technology of Hebei Province, College of Chemistry and Environmental Science, Hebei University, Baoding 071002, China;* Email: zhangbingbing@hbu.edu.cn

Authors

Ya Yang − *Key Laboratory of Medicinal Chemistry and Molecular Diagnosis of the Ministry of Education, Key Laboratory of Analytical Science and Technology of Hebei Province, College of Chemistry and Environmental Science, Hebei University, Baoding 071002, China*

Xiaowen Wu − *Key Laboratory of Medicinal Chemistry and Molecular Diagnosis of the Ministry of Education, Key Laboratory of Analytical Science and Technology of Hebei Province, College of Chemistry and Environmental Science, Hebei University, Baoding 071002, China*

Ming-Hsien Lee − *Department of Physics, Tamkang University, New Taipei City 25137, Taiwan*

Complete contact information is available at: https://pubs.acs.org/10.1021/acs.chemmater.9b04842

Author Contributions

The manuscript was written through contributions of all the authors.

Notes

The authors declare no competing financial interest.

■ ACKNOWLEDGMENTS

This work was supported by the National Natural Science Foundation of China (Grant Nos. 51872324, 21763026, and 51702356), the Natural Science Foundation of Hebei Province (Grant Nos. E2019201049 and B2019201433), and the Advanced Talents Incubation Program of the Hebei University (801260201293).

■ REFERENCES

(1) Tran, T. T.; Yu, H.; Rondinelli, J. M.; Poeppelmeier, K. R.; Halasyamani, P. S. Deep Ultraviolet Nonlinear Optical Materials. *Chem. Mater.* **2016**, *28*, 5238−5258.

(2) Chung, I.; Kanatzidis, M. G. Metal Chalcogenides: A Rich Source of Nonlinear Optical Materials. *Chem. Mater.* **2014**, *26*, 849−869.

(3) Mutailipu, M.; Zhang, M.; Yang, Z.; Pan, S. Targeting the Next Generation of Deep-Ultraviolet Nonlinear Optical Materials: Expanding from Borates to Borate Fluorides to Fluorooxoborates. *Acc. Chem. Res.* **2019**, *52*, 791−801.

(4) Shen, Y. G.; Zhao, S. G.; Luo, J. H. The role of cations in second-order nonlinear optical materials based on π-conjugated $[BO_3]^{3-}$ groups. *Coord. Chem. Rev.* **2018**, *366*, 1−28.

(5) Zou, G.; Jo, H.; Lim, S.-J.; You, T.-S.; Ok, K. M. $Rb_3VO(O_2)_2CO_3$: A Four-in-One Carbonatoperoxovanadate Exhibiting an Extremely Strong Second-Harmonic Generation Response. *Angew. Chem., Int. Ed.* **2018**, *57*, 8619−8622.

(6) Luo, M.; Liang, F.; Song, Y.; Zhao, D.; Xu, F.; Ye, N.; Lin, Z. $M_2B_{10}O_{14}F_6$ (M = Ca, Sr): Two Noncentrosymmetric Alkaline Earth Fluorooxoborates as Promising Next-Generation Deep-Ultraviolet Nonlinear Optical Materials. *J. Am. Chem. Soc.* **2018**, *140*, 3884−3887.

(7) Chen, J.; Xiong, L.; Chen, L.; Wu, L.-M. $Ba_2NaClP_2O_7$: Unprecedented Phase Matchability Induced by Symmetry Breaking and Its Unique Fresnoite-Type Structure. *J. Am. Chem. Soc.* **2018**, *140*, 14082−14086.

(8) Xia, Z. G.; Poeppelmeier, K. R. Chemistry-inspired adaptable framework structures. *Acc. Chem. Res.* **2017**, *50*, 1222−1230.

(9) Xia, M. J.; Jiang, X. X.; Lin, Z. S.; Li, R. K. "All-Three-in-One": A New Bismuth−Tellurium−Borate Bi_3TeBO_9 Exhibiting Strong Second Harmonic Generation Response. *J. Am. Chem. Soc.* **2016**, *138*, 14190−14193.

(10) Ok, K. M. Toward the rational design of novel non-centrosymmetric materials: factors influencing the framework structures. *Acc. Chem. Res.* **2016**, *49*, 2774−2785.

(11) Mao, F. F.; Hu, C. L.; Chen, J.; Mao, J. G. A Series of Mixed-Metal Germanium Iodates as Second-Order Nonlinear Optical Materials. *Chem. Mater.* **2018**, *30*, 2443−2452.

(12) Liang, F.; Kang, L.; Gong, P. F.; Lin, Z. S.; Wu, Y. C. Rational design of deep-ultraviolet nonlinear optical materials in fluorooxoborates: toward optimal planar configuration. *Chem. Mater.* **2017**, *29*, 7098−7102.

(13) Wu, H. P.; Pan, S. L.; Poeppelmeier, K. R.; Li, H. Y.; Jia, D. Z.; Chen, Z. H.; Fan, X. Y.; Yang, Y.; et al. $K_3B_6O_{10}Cl$: a new structure analogous to perovskite with a large SHG response and deep UV absorption edge. *J. Am. Chem. Soc.* **2011**, *133*, 7786−7790.

(14) Wang, X. F.; Wang, Y.; Zhang, B. B.; Zhang, F. F.; Yang, Z. H.; Pan, S. L. CsB_4O_6F: a congruent-melting deep-ultraviolet nonlinear optical material by combining superior functional units. *Angew. Chem., Int. Ed.* **2017**, *56*, 14119−14123.

(15) Shi, G. Q.; Wang, Y.; Zhang, F. F.; Zhang, B. B.; Yang, Z. H.; Hou, X. L.; Pan, S. L.; Poeppelmeier, K. R. Finding the next deep-ultraviolet nonlinear optical material: $NH_4B_4O_6F$. *J. Am. Chem. Soc.* **2017**, *139*, 10645−10648.

(16) Huang, Y.; Meng, X. G.; Gong, P. F.; Lin, Z. S.; Chen, X. G.; Qin, J. G. A study on $K_2SbF_2Cl_3$ as a new mid-IR nonlinear optical material: new synthesis and excellent properties. *J. Mater. Chem. C* **2015**, *3*, 9588−9593.

(17) Kim, H. G.; Tran, T. T.; Choi, W.; You, T. S.; Halasyamani, P. S.; Ok, K. M. Two New Non-centrosymmetric n = 3 Layered Dion−Jacobson Perovskites: Polar $RbBi_2Ti_2NbO_{10}$ and Nonpolar $CsBi_2Ti_2TaO_{10}$. *Chem. Mater.* **2016**, *28*, 2424−2432.

(18) Zou, G. H.; Lin, C. S.; Jo, H.; Nam, G.; You, T. S.; Ok, K. M. Pb_2BO_3Cl: A Tailor-Made Polar Lead Borate Chloride with Very Strong Second Harmonic Generation. *Angew. Chem., Int. Ed.* **2016**, *55*, 12078−12082.

(19) Zhao, S. G.; Kang, L.; Shen, Y. G.; Wang, X. D.; Asghar, M. A.; Lin, Z. S.; Xu, Y. Y.; Zeng, S. Y.; Hong, M. C.; Luo, J. H. Designing a Beryllium-Free Deep-Ultraviolet Nonlinear Optical Material without a Structural Instability Problem. *J. Am. Chem. Soc.* **2016**, *138*, 2961−2964.

(20) Lan, H. C.; Liang, F.; Jiang, X. X.; Zhang, C.; Yu, H. H.; Lin, Z. S.; Zhang, H. J.; Wang, J. Y.; Wu, Y. C. Pushing Nonlinear Optical Oxides into the Mid-Infrared Spectral Region Beyond 10 μm: Design, Synthesis, and Characterization of $La_3SnGa_5O_{14}$. *J. Am. Chem. Soc.* **2018**, *140*, 4684−4690.

(21) Kang, L.; Zhou, M. L.; Yao, J. Y.; Lin, Z. S.; Wu, Y. C.; Chen, C. T. Metal thiophosphates with good mid-infrared nonlinear optical performances: A first-principles prediction and analysis. *J. Am. Chem. Soc.* **2015**, *137*, 13049−13059.

(22) Bera, T. K.; Jang, J. I.; Ketterson, J. B.; Kanatzidis, M. G. Strong Second Harmonic Generation from the Tantalum Thioarsenates $A_3Ta_2AsS_{11}$ (A = K and Rb). *J. Am. Chem. Soc.* **2009**, *131*, 75−77.

(23) Luo, Z. Z.; Lin, C. S.; Cui, H. H.; Zhang, W. L.; Zhang, H.; Chen, H.; He, Z. Z.; Cheng, W. D. $PbGa_2MSe_6$ (M = Si, Ge): Two Exceptional Infrared Nonlinear Optical Crystals. *Chem. Mater.* **2015**, *27*, 914−922.

(24) Li, S. F.; Jiang, X. M.; Liu, B. W.; Yan, D.; Lin, C. S.; Zeng, H. Y.; Guo, G. C. Superpolyhedron-Built Second Harmonic Generation Materials Exhibit Large Mid-Infrared Conversion Efficiencies and

High Laser-Induced Damage Thresholds. *Chem. Mater.* **2017**, *29*, 1796−1804.
(25) Brant, J. A.; Clark, D. J.; Kim, Y. S.; Jang, J. I.; Zhang, J. H.; Aitken, J. A. Li_2CdGeS_4, A Diamond-Like Semiconductor with Strong Second-Order Optical Nonlinearity in the Infrared and Exceptional Laser Damage Threshold. *Chem. Mater.* **2014**, *26*, 3045−3048.
(26) Liu, B. W.; Zeng, H. Y.; Jiang, X. M.; Wang, G. E.; Li, S. F.; Xu, L.; Guo, G. C. $[A_3X][Ga_3PS_8]$ (A = K, Rb; X = Cl, Br): promising IR non-linear optical materials exhibiting concurrently strong second-harmonic generation and high laser induced damage thresholds. *Chem. Sci.* **2016**, *7*, 6273−6277.
(27) Liu, B. W.; Zhang, M. Y.; Jiang, X. M.; Li, S. F.; Zeng, H. Y.; Wang, G. Q.; Fan, Y. H.; Su, Y. F.; Li, C. S.; Guo, G. C.; Huang, J. S. Large Second-Harmonic Generation Responses Achieved by the Dimeric $[Ge_2Se_4(\mu\text{-}Se_2)]^{4-}$ Functional Motif in Polar Polyselenides $A_4Ge_4Se_{12}$ (A = Rb, Cs). *Chem. Mater.* **2017**, *29*, 9200−9207.
(28) Li, C.; Yin, W. L.; Gong, P. F.; Li, X. S.; Zhou, M. L.; Mar, A.; Lin, Z. S.; Yao, J. Y.; Wu, Y. C.; Chen, C. T. Trigonal Planar $[HgSe_3]^{4-}$ Unit: A New Kind of Basic Functional Group in IR Nonlinear Optical Materials with Large Susceptibility and Physicochemical Stability. *J. Am. Chem. Soc.* **2016**, *138*, 6135−6138.
(29) Zhou, M. L.; Yang, Y.; Guo, Y. W.; Lin, Z. S.; Yao, J. Y.; Wu, Y. C.; Chen, C. T. Hg-Based Infrared Nonlinear Optical Material $KHg_4Ga_5Se_{12}$ Exhibits Good Phase-Matchability and Exceptional Second Harmonic Generation Response. *Chem. Mater.* **2017**, *29*, 7993−8002.
(30) Shi, Y. F.; Chen, Y. K.; Chen, M. C.; Wu, L. M.; Lin, H.; Zhou, L. J.; Chen, L. Strongest Second Harmonic Generation in the Polar R_3MTQ_7 Family: Atomic Distribution Induced Nonlinear Optical Cooperation. *Chem. Mater.* **2015**, *27*, 1876−1884.
(31) Kang, L.; Liang, F.; Jiang, X. X.; Lin, Z. S.; Chen, C. T. First-Principles Design and Simulations Promote the Development of Nonlinear Optical Crystals. *Acc. Chem. Res.* **2019**, 209−217.
(32) Liang, F.; Kang, L.; Lin, Z. S.; Wu, Y. C. Mid-infrared nonlinear optical materials based on metal chalcogenides: structure−property relationship. *Cryst. Growth Des.* **2017**, *17*, 2254−2289.
(33) Liu, B. W.; Zhang, M. J.; Zhao, Z. Y.; Zeng, H. Y.; Zheng, F. K.; Guo, G. C.; Huang, J. S. Synthesis, structure, and optical properties of the quaternary diamond-like compounds I_2−II−IV−VI_4 (I = Cu; II = Mg; IV = Si, Ge; VI = S, Se). *J. Solid State Chem.* **2013**, *204*, 251−256.
(34) Zhang, M. J.; Jiang, X. M.; Zhou, L. J.; Guo, G. C. Two phases of Ga_2S_3: promising infrared second-order nonlinear optical materials with very high laser induced damage thresholds. *J. Mater. Chem. C* **2013**, *1*, 4754−4760.
(35) Liu, B. W.; Jiang, X. M.; Li, B. X.; Zeng, H. Y.; Guo, G. C. $Li[LiCs_2Cl][Ga_3S_6]$: A Nanoporous Framework of GaS_4 Tetrahedra with Excellent Nonlinear Optical Performance. *Angew. Chem., Int. Ed.* **2019**, DOI: 10.1002/anie.201912416.
(36) Dunitz, J. D.; Bernstein, J. Disappearing Polymorphs. *Acc. Chem. Res.* **1995**, *28*, 193−200.
(37) Cong, R. H.; Yang, T.; Lin, Z. S.; Bai, L.; Ju, J.; Liao, F. H.; Wang, Y. X.; Lin, J. H. Rare Earth Induced Formation of δ-BiB_3O_6 at Ambient Pressure with Strong Second Harmonic Generation. *J. Mater. Chem.* **2012**, *22*, 17934−17941.
(38) Emme, H.; Huppertz, H. High-Pressure Preparation, Crystal Structure, and Properties of α-$(RE)_2B_4O_9$ (RE = Eu, Gd, Tb, Dy): Oxoborates Displaying a New Type of Structure with Edge-Sharing BO_4 Tetrahedra. *Chem. - Eur. J.* **2003**, *9*, 3623−3633.
(39) Cong, R. H.; Zhu, J. L.; Wang, Y. X.; Yang, T.; Liao, F. H.; Jin, C. Q.; Lin, J. H. Phase Transitions Among Four BiB_3O_6 Polymorphs: A Detailed Investigation. *CrystEngComm* **2009**, *11*, 1971−1978.
(40) Yu, H. W.; Wu, H. P.; Jing, Q.; Yang, Z. H.; Halasyamani, P. S.; Pan, S. L. Polar Polymorphism: α-, β-, and γ-$Pb_2Ba_4Zn_4B_{14}O_{31}$−Synthesis, Characterization, and Nonlinear Optical Properties. *Chem. Mater.* **2015**, *27*, 4779−4788.
(41) Liang, F.; Kang, L.; Li, Z. S.; Wu, Y. C.; Chen, C. T. Analysis and prediction of mid-IR nonlinear optical metal sulfides with diamond-like structures. *Coord. Chem. Rev.* **2017**, *333*, 57−70.
(42) Rosmus, K. A.; Brant, J. A.; Wisneski, S. D.; Clark, D. J.; Kim, Y. S.; Jang, J. I.; Brunetta, C. D.; Zhang, J. H.; Srnec, M. N.; Aitken, J. A. Optical Nonlinearity in Cu_2CdSnS_4 and α/β-Cu_2ZnSiS_4: Diamond-like Semiconductors with High Laser-Damage Thresholds. *Inorg. Chem.* **2014**, *53*, 7809−7811.
(43) Devlin, K. P.; Glaid, A. J.; Brant, J. A.; Zhang, J. H.; Srnec, M. N.; Clark, D. J.; Kim, Y. S.; Jang, J. I.; Daley, K. R.; Moreau, M. A.; Madura, J. D.; Aitken, J. A. Polymorphism and second harmonic generation in a novel diamond-like semiconductor: Li_2MnSnS_4. *J. Solid State Chem.* **2015**, *231*, 256−266.
(44) Nian, L. Y.; Huang, J. B.; Wu, K.; Su, Z.; Yang, Z. H.; Pan, S. L. $BaCu_2M^{IV}Q_4$ (M^{IV} = Si, Ge, and Sn; Q = S, Se): synthesis, crystal structures, optical performances and theoretical calculations. *RSC Adv.* **2017**, *7*, 29378−29385.
(45) Assoud, A.; Soheilnia, N.; Kleinke, H. New quaternary barium copper/silver selenostannates: different coordination spheres, metal-metal interactions, and physical properties. *Chem. Mater.* **2005**, *17*, 2255−2261.
(46) Hersh, P. A. Wide band gap semiconductors and insulators: synthesis, processing and characterization. PhD Dissertation, Oregon State University, 2008.
(47) Teske, C. L. Darstellung und Kristallstruktur von Cu_2SrSnS_4. *Z. Anorg. Allg. Chem.* **1976**, *419*, 67−76.
(48) Chen, H.; Liu, P. F.; Li, B. X.; Lin, H.; Wu, L. M.; Wu, X. T. Experimental and theoretical studies on the NLO properties of two quaternary non-centrosymmetric chalcogenides: $BaAg_2GeS_4$ and $BaAg_2SnS_4$. *Dalton Trans.* **2018**, *47*, 429−437.
(49) Wu, K.; Yang, Z. H.; Pan, S. L. Na_2BaMQ_4 (M = Ge, Sn; Q = S, Se): Infrared Nonlinear Optical Materials with Excellent Performances and that Undergo Structural Transformations. *Angew. Chem., Int. Ed.* **2016**, *55*, 6713−6715.
(50) Parasyuk, O. V.; Piskach, L. V.; Olekseyuk, I. D.; Pekhnyo, V. I. The quasi-ternary system (Ag_2S)-(CdS)-(GeS_2) and the crystal structure of Ag_2CdGeS_4. *J. Alloys Compd.* **2005**, *397*, 95−98.
(51) Brunetta, C. D.; Minsterman, W. C., III; Lake, C. H.; Aitken, J. A. Cation ordering and physicochemical characterization of the quaternary diamond-like semiconductor Ag_2CdGeS_4. *J. Solid State Chem.* **2012**, *187*, 177−185.
(52) Doverspike, K.; Kershaw, R.; Dwight, K.; Wold, A. Preparation and properties of the system $Cu_2Zn_{1-x}Fe_xGeS_4$. *Mater. Res. Bull.* **1988**, *23*, 959−964.
(53) Parasyuk, O. V.; Piskach, L. V.; Romanyuk, Y. E.; Olekseyuk, I. D.; Zaremba, V. I.; Pekhnyo, V. I. Phase relations in the quasi-binary (Cu_2GeS_3)-(ZnS) and quasi-ternary (Cu_2S)-Zn (Cd)S-(GeS_2) systems and crystal structure of Cu_2ZnGeS_4. *J. Alloys Compd.* **2005**, *397*, 85−94.
(54) Hamdi, M.; Lafond, A.; Guillot-Deudon, C.; Hlel, F.; Gargouri, M.; Jobic, S. Crystal chemistry and optical investigations of the $Cu_2Zn(Sn, Si)S_4$ series for photovoltaic applications. *J. Solid State Chem.* **2014**, *220*, 232−237.
(55) Ritscher, A.; Hoelzel, M.; Lerch, M. The order-disorder transition in Cu_2ZnSnS_4 - A neutron scattering investigation. *J. Solid State Chem.* **2016**, *238*, 68−73.
(56) Nian, L. Y.; Wu, K.; He, G. J.; Yang, Z. H.; Pan, S. L. Effect of Element Substitution on Structural Transformation and Optical Performances in $I_2BaM^{IV}Q_4$ (I = Li, Na, Cu, and Ag; M^{IV} = Si, Ge, and Sn; Q = S and Se). *Inorg. Chem.* **2018**, *57*, 3434−3442.
(57) Zhu, T.; Huhn, W. P.; Wessler, G. C.; Shin, D.; Saparov, B.; Mitzi, D. B.; Blum, V. I_2−II−IV−VI_4 (I = Cu, Ag; II = Sr, Ba; IV = Ge, Sn; VI = S, Se): Chalcogenides for Thin-Film Photovoltaics. *Chem. Mater.* **2017**, *29*, 7868−7879.
(58) Tampier, M.; Johrendt, D. Neue azentrische Selenogermanate. I. Kristallstrukturen und chemische Bindung von AM_2GeSe_4 (A = Sr, Ba; M = Cu, Ag). *Z. Anorg. Allg. Chem.* **2001**, *627*, 312−320.
(59) Boyd, G. D.; Buehler, E.; Storz, F. G. Linear and Nonlinear Optical Properties of $ZnGeP_2$ and CdSe. *Appl. Phys. Lett.* **1971**, *18*, 301−304.

(60) Bhar, G. C.; Smith, R. C. Optical Properties of II−IV−V_2 and I−III−VI_2 crystals with Particular Reference to Transmission Limits. *Phys. Status Solidi A* **1972**, *13*, 157−168.
(61) Perdew, J. P.; Burke, K.; Ernzerhof, M. Generalized Gradient Approximation Made Simple. *Phys. Rev. Lett.* **1996**, *77*, 3865−3870.
(62) Wu, K.; Chu, Y.; Yang, Z. H.; Pan, S. L. $A_2SrM^{IV}S_4$ (A. = Li, Na; M^{IV} = Ge, Sn) concurrently exhibiting wide bandgaps and good nonlinear optical responses as new potential infrared nonlinear optical materials. *Chem. Sci.* **2019**, *10*, 3963−3968.
(63) Isaenko, L. I.; Vasilyeva, I. G. Nonlinear $LiB^{III}C_2{}^{YI}$ crystals for mid-IR and far-IR: Novel aspects in crystal growth. *J. Cryst. Growth* **2008**, *310*, 1954−1960.
(64) Isaenko, L.; Vasilyeva, I.; Merkulov, A.; Yelisseyev, A.; Lobanov, S. Growth of new nonlinear crystals $LiMX_2$ (M = Al, In, Ga; X = S, Se, Te) for the mid-IR optics. *J. Cryst. Growth* **2005**, *275*, 217−223.
(65) Isaenko, L.; Yelisseyev, A.; Lobanov, S.; Titov, A.; Petrov, V.; Zondy, J. J.; Krinitsin, P.; Merkulov, A.; Vedenyapin, V.; Smirnova. Growth and properties of $LiGaX_2$ (X = S, Se, Te) single crystals for nonlinear optical applications in the mid-IR. *Cryst. Res. Technol.* **2003**, *38*, 379−387.
(66) Petrov, V.; Zondy, J. J.; Bidault, O.; Isaenko, L.; Vedenyapin, V.; Yelisseyev, A.; Chen, W. D.; Tyazhev, A.; Lobanov, S.; Marchev, G.; Kolker, D. Optical, thermal, electrical, damage, and phase-matching properties of lithium selenoindate. *J. Opt. Soc. Am. B* **2010**, *27*, 1902−1927.
(67) Lin, X. S.; Zhang, G.; Ye, N. Growth and Characterization of $BaGa_4S_7$: A New Crystal for Mid-IR Nonlinear Optics. *Cryst. Growth Des.* **2009**, *9*, 1186−1189.
(68) Lin, H.; Zhou, L. J.; Chen, L. Sulfides with Strong Nonlinear Optical Activity and Thermochromism: $ACd_4Ga_5S_{12}$ (A = K, Rb, Cs). *Chem. Mater.* **2012**, *24*, 3406−3414.

https://dx.doi.org/10.1021/acs.chemmater.9b04842
Chem. Mater. 2020, 32, 1281−1287